Mechanisms of Oxidation of 1,2,5-Trimethylpyrrole: Kinetic, Spectroscopic, and Electrochemical Studies

Bruce Beaver and Yun Teng

Department of Chemistry and Biochemistry, Duquesne University, Pittsburgh, Pennsylvania 15282

Philippe Guiriec and Philippe Hapiot

Laboratoire d'Electrochimie Moleculaire, Unite Mixte de Recherche CNRS No 7591, Universite Denis Diderot (Paris 7), case courier No 7107, 2 place Jussieu, 75251 Paris Cedex 05, France

P. Neta*

Physical and Chemical Properties Division, National Institute of Standards and Technology, Gaithersburg, Maryland 20899

Received: January 22, 1998; In Final Form: May 14, 1998

The oxidation of 1,2,5-trimethylpyrrole (TMP) in aqueous and organic solvents is studied by various techniques. Heating oxygenated chlorobenzene solutions of TMP results in autoxidation that is initiated via reaction of TMP with O_2 and partly propagated via oxidation of TMP by a TMP-derived peroxyl radical. In radiolytic experiments, TMP is oxidized rapidly by $Br_2^{\bullet-}$ ($k = 2.3 \times 10^9$ L mol^{-1} s^{-1}), $I_2^{\bullet-}$ ($k = 5.1 \times 10^8$ L mol^{-1} s^{-1}), $CCl_3O_2^{\bullet}$ ($k = 5 \times 10^8$ L mol^{-1} s^{-1}), and $N_3^{\bullet}$ radicals in aqueous solutions and by peroxyl radicals in organic solvents. One-electron oxidation forms the radical cation, which exhibits significant absorption in the UV ($\lambda_{max} \sim 270$ nm, $\epsilon \sim 1300$ L mol^{-1} cm^{-1}) and weaker absorptions in the visible range. This species undergoes rapid dimerization ($2k \sim 5 \times 10^8$ L mol^{-1} s^{-1}), and the dimer is very easily oxidized to a stable product absorbing around 460 nm. NMR analysis of the product formed in irradiated CH_2Cl_2 solutions is in accord with a dication of dimeric TMP. Other products are also formed under different conditions, probably resulting from addition of peroxyl radicals to the pyrrole ring. In cyclic voltammetry experiments at low scan rates, an irreversible peak at a potential of 0.72 V vs SCE is found for oxidation of TMP in acetonitrile solutions, and a stable product absorbing at 460 nm is formed. The formation of this product involves the transfer of more than one electron per TMP monomer. At very high scan rates, a reversible oxidation step is observed, from which a redox potential of 0.87 V vs SCE is derived for the couple TMP/TMP$^{\bullet+}$. Several mechanisms are suggested for the consumption of O_2 by TMP in organic solvents, including electron transfer and σ-bonding via peroxyl radical addition.

Introduction

Alkylpyrroles have been shown to undergo thermal reaction with O_2 in polar aprotic solvents via a self-initiated autoxidation process which is not inhibited by phenolic antioxidants such as butylated hydroxytoluene (BHT).[1] In a similar fashion, the autoxidation of 2,5-dimethylpyrrole (DMP) at 120 °C in a nonpolar solvent is only partially inhibited by BHT.[2] To account for the lack of an effect of phenolic antioxidants on the rate of pyrrole autoxidation, it has been proposed that the autoxidation is initiated by a rate-limiting step involving an electron transfer from the pyrrole to O_2 and is propagated by rapid reactions of the pyrrole radical cation and of superoxide, without the intermediacy of peroxyl radicals, to yield a complex mix of final oxidation products.[3] This mechanism has been described as electron-tranfer-initiated oxygenation (ETIO) in order to distingish it from the more commonly encountered peroxyl-radical chain mechanism for autoxidation.[4] ETIO reactions of various electron-rich molecules that are indigenous to many petroleum products have been suggested to be involved in their oxidative degradation.[5] Most recently it has been shown that the ETIO reactions of various arylphosphines in nonpolar solvents lead to oxygen-scavenging properties which may prove useful in the thermal oxidative stability of jet fuels.[6,7] To further explore the ETIO hypothesis, we have performed kinetic studies on a representative electron-rich molecule, 1,2,5-trimethylpyrrole (TMP), and to help elucidate the mechanism of oxidation, we studied this process by electrochemical and radiolytic techniques in various environments.

Numerous electrochemical studies have been carried out on the oxidation of pyrroles, showing that the initial radical cations lead to formation of dimers and subsequently polymers.[8] These processes were studied mainly with pyrroles that are unsubstituted at the 2,5-positions, where dimerization and polymerization take place. No polymers were formed when the 2,5-positions were alkylated, and thus it was assumed that dimerization also is less likely in such compounds.[9]

Previous calculations and electron spin resonance measurements on pyrrole radical cations have shown that the unpaired electron density is much higher at the α-positions than at the β-positions.[10] This leads to dimerization of the radical cations predominantly through the α-positions. However, when $\beta-\beta$ couplings occur, these are responsible for a loss of conjugation in the polymer chain and a decrease of its conductivity.[11] To

S1089-5639(98)00832-9 CCC: $15.00
Published on Web 07/01/1998

predict the behavior of the radical cation of TMP, we have calculated its geometry and spin densities by full optimization of the geometry using density functional theory (DFT) with the B3LYP[12] functional using the 6-31G* basis set;[13] calculations were performed with the Gaussian 94W package.[14] We found values of 0.47 and 0.07 at the α- and β-positions, respectively. Because the two α-positions are hindered by methyl groups and also by the substitution on the nitrogen, coupling through the β-positions is likely to occur even if the spin density at the β-position is much lower than that at the α-position. However, besides the possible β−β coupling, recent results obtained with substituted oligothiophene[15] or oligopyrrole[9] radical cations have shown that α−α couplings take place even when the α-positions are blocked not only with methyl groups but also with bulkier groups such as $Si(CH_3)_3$. When the substituents can be readily eliminated after dimerization, as in the case of $Si(CH_3)_3$ groups, the linear polymer obtained after the oxidation of the oligomer has better conjugation length and fewer defects.[16] In this case, the oxidation mechanism involves the hindered coupling between two silylated radical cations followed by nucleophilic assisted elimination of two $Si(CH_3)_3^+$ moieties.[17] When the two substituents are methyl groups, the protonated dimer produced after the coupling step does not readily lead to the corresponding dimer and the C−C bond can break to give back the monomeric radical cation, leading to a reversible dimerization, i.e., to an equilibrium between the radical cation $A^{\bullet+}$ and the protonated dimer A_2^{2+}. However, at long times A_2^{2+} can decay by nucleophilic attack of impurities in the solvent.[15] Thus, two types of competitive pathways can be expected: (a) hindered α−α coupling (reversible) followed by nucleophilic attack or (b) β−β coupling followed by deprotonation (rearomatization). The present study shows that $TMP^{\bullet+}$ undergoes rapid dimerization by bonding at the β-position, followed by rapid oxidation of the dimer to a stable dication, but no polymerization. Formation and reactions of the intermediate species were studied by pulse radiolysis and electrochemistry.

Experimental Section

1,2,5-Trimethylpyrrole (TMP) was obtained from Aldrich[18] and the solvents from Mallinckrodt. They were obtained in the highest available purity and were used as received. The inorganic materials also were from Mallinckrodt, and water was purified with a Millipore Super-Q system. Solutions were prepared immediately before irradiation and were protected from light to prevent UV photolysis. Gamma radiolysis experiments were carried out in a Gammacell 220 ^{60}Co source with a dose rate of 0.79 Gy s^{-1}. The radiolytic yield was determined from the changes in absorbance following irradiation with various doses. The observation of transient species and the determination of their kinetic behavior were performed with the NIST Febetron-based pulse radiolysis apparatus. Solutions were irradiated with a 50 ns pulse of 2 MeV electrons, and the formation and decay of transient species were followed by kinetic spectrophotometry at various wavelengths. The dose per pulse was generally between 5 and 50 Gy. Other details of the apparatus were given before.[7] All experiments were performed at room temperature, 20 ± 2 °C. The overall standard uncertainties are estimated to be ±5% for the *G* values and ±15% for the rate constants, unless otherwise indicated.

Electrochemical experiments were performed with a three-electrode setup using a platinum counter electrode and a calomel reference electrode. Acetonitrile (Merck, Uvasol, less than 0.01% of water) was used with tetraethylammonium tetrafluoroborate electrolyte (Fluka, puriss.). Solutions were kept under Ar. For low scan rate cyclic voltammetry using millimetric electrodes (1 mm diameter gold or carbon disk electrodes), the electrochemical instrumentation consisted of a PAR model 175 Universal programmer and a home-built potentiostat equipped with a positive feedback compensation device.[19] The data were acquired with 310 Nicolet oscilloscope. Fast electrochemical experiments were performed using 10 μm diameter disk platinum ultramicroelectrodes. Equipment and procedures were the same as previously published.[20] The potential values reported are averages of several reproducible experiments; all potentials were internally calibrated against the ferrocene/ferricinium couple ($E = 0.405$ V vs SCE) for each experiment. Simulations of the cyclic voltamograms were performed using Bas DigiSim 2.0 (Bioanalytical Systems).

Spectroelectrochemical experiments were performed with a capillary slit cell for UV−vis spectroscopy using gold-LIGA structures as an optically transparent electrode.[21] The gold-LIGA structure was fixed in a capillary slit of 150 μm. A silver wire coated with silver chloride was used as reference electrode.

For the autoxidation studies, TMP was distilled prior to use and experimental details are as described before.[2]

TABLE 1: Initial Rates for the Self-Initiated Autoxidation of 1,2,5-Trimethylpyrrole (TMP) in Chlorobenzene at 131 °C under Different Conditions

expt	[TMP] (mol L^{-1})	[BHT] (mol L^{-1})	% O_2 saturation	[TPP] (mol L^{-1})	initial rate ($\times 10^6$ mol L^{-1} min^{-1})
1	0.022		20		7.5 ± 0.6[a]
2	0.022		100		31.8 ± 2.9
3	0.086		100		146 ± 12
4	0.022	0.022	100		15.6 ± 4.1
5	0.022	0.044	100		16.6 ± 1.2
6	0.022	0.022	20		3.9 ± 0.8
7	0.043	0.022	100		30.1 ± 1.3
8	0.022		100	0.022	76.4 ± 1.5
9	0.022	0.022	100	0.022	45.5 ± 1.7
10	0.022	0.088	100	0.022	37.0 ± 3.6
11	0.022	0.088	20	0.022	8.8 ± 1.7
12	0.086	0.088	100	0.022	148 ± 9

[a] Confidence limits were calculated using $X \pm (ts/[n^{1/2}])$, where X is the mean of a number of measurements, n is the standard deviation, and t is the student t variate for the 95% limit of confidence.

Results and Discussion

Autoxidation Studies. Heating an O_2-saturated chlorobenzene solution of TMP at 131 °C results in a self-initiated[22] autoxidation which can be only partially inhibited by the phenolic antioxidant BHT (Table 1). Comparison of experiments 2, 4, and 5 reveals that only about 50% of the TMP autoxidation can be inhibited by the BHT. This observation suggests that approximately one-half of the TMP autoxidation can be accounted for by operation of a peroxyl radical chain mechanism. Consistent with this suggestion is the observation that the presence of triphenylphosphine (TPP) results in an increase in the rate of TMP autoxidation (experiments 2 vs 8). Presumably, TPP is reacting with the TMP peroxyl radical ($TMPOO^{\bullet}$) to yield the more reactive TMP alkoxyl radical ($TMPO^{\bullet}$) and triphenylphosphine oxide (TPPO).[23] Also consistent with this suggestion is the observation that the addition of increasing amounts of BHT is not very effective in inhibiting the action of the reactive TMP alkoxyl radical (experiments 4 vs 9 and 10).

Various experiments in Table 1 indicate that the rate law for TMP autoxidation is similar in the presence of BHT singly and in the BHT/TPP combination, being 0.9 order in both O_2 and

SCHEME 1

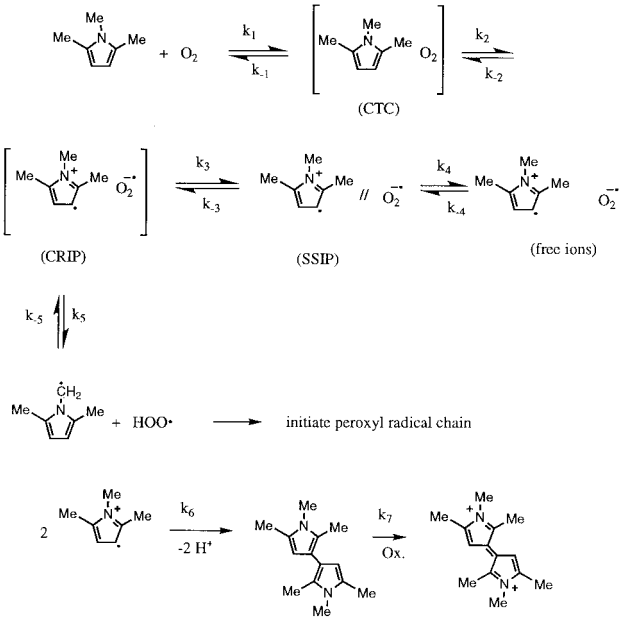

TMP (experiments 4, 6, and 7; 9, 11, and 12). In the absence of any additives the observed rate law is approximately 0.9 in O_2 and 1.1 in TMP (experiments 1−3). In addition, we note that prolonged autoxidation of the TMP solutions results in the initially colorless solution becoming dark brown.

Scheme 1 outlines an ETIO mechanism that is consistent with all of our experimental data. In step 1, TMP reversibly forms a charge-transfer complex (CTC) with oxygen. Spectroscopic evidence has been presented that is consistent with 2,5-dimethylpyrrole forming such complexes in dodecane.[24] Rate-limiting thermal electron transfer from TMP to oxygen yields a contact radical ion pair (CRIP) in step 2. Results from picosecond laser-flash photolytic studies[25] allow us to propose the existence of such an ion pair as an important reactive intermediate in this system. Ion pair dynamics are largely controlled by the stability of the ions formed and by solvent polarity.[25] In fact, with stable ions, extensive formation of solvent-separated ion pairs (SSIP) in dichloromethane has been demonstrated. The free ions subsequently formed may react by reverse electron transfer, by addition, or by self-reactions. It is known from pulse radiolysis[26] and electrochemical[27] studies that certain radical cations can rapidly dimerize. Analogously, we propose a similar step between two TMP radical cations in step 6. Facile oxidation of the dimer would be expected to produce chromophores that absorb in the visible region (as observed in the radiolytic and electrochemical experiments described below). Another possible reaction for the TMP radical cations is combination with $O_2^{\bullet-}$ to produce a hydroperoxide zwitterion (not shown in Scheme 1), which will decompose to yield different final products. This route may compete with the reverse electron transfer, as suggested for tyrosyl[28] and for a nitrogen-centered radical of a tryptophan derivative.[29]

We propose that the reactivity of the CRIP determines the nature of the autoxidation. In our system, k_3 and k_5 are competitive with rapid back electron transfer, k_{-2}. Step 5 involves deprotonation of the TMP radical cation by superoxide to form the TMP radical and the hydroperoxyl radical. It is well-known that alkyl-substituted aromatic radical cations are acidic[30] and can be deprotonated in aprotic solvents by the superoxide ion.[31] The hydroperoxyl radical will either undergo dismutation, with another hydroperoxyl or with superoxide, or oxidize another TMP molecule.

SCHEME 2

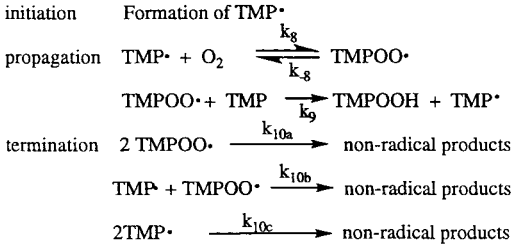

The TMP radical generated by step 5 will react with oxygen to yield TMPOO• and initiate the peroxyl radical chain mechanism of Scheme 2. Owing to the high temperature in our experiments, the presumed stability of the TMP radical, and the kinetic orders observed for this chain reaction, we propose that the oxygen addition in step 8 is reversible. Step 9 is a rate-limiting reaction which may involve either hydrogen atom abstraction to yield a hydroperoxide and another TMP radical (as formulated in Scheme 2) or addition to form a different TMP radical. Owing to the complexity in the nature of pyrrole oxidation products,[5] we cannot distinguish between these two possibilities. Any hydroperoxide formed in step 9 will oxidize another TMP molecule.[32] If step 8 is reversible, three termination pathways are available as shown in steps 10a, 10b, and 10c. As shown in the Appendix, standard steady-state assumptions allow derivation of eq 11 for the rate law of the peroxyl chain depicted in Scheme 2.

$$-\mathrm{d[TMP]}/\mathrm{d}t = k_9 K_1^{1/2} K_2^{1/2} [\mathrm{TMP}]^{3/2} [\mathrm{O_2}]^{3/2} / \{k_{10a} k_8^2 [\mathrm{O_2}]^2 + k_{10b} k_8 k_{-8} [\mathrm{O_2}] + k_{10c} k_{-8} 2\}^{1/2} \quad (11)$$

Equation 11 has a complex order dependence on [O_2] and a 3/2-order dependence on [TMP]. In the absence of BHT we have determined that there is a 0.9-order dependence on [O_2] and a 1.1-order dependence on [TMP]. Presumably Schemes 1 and 2 are operating concurrently in the absence of BHT. Since the ETIO mechanism in Scheme 1 is expected to exhibit a first-order dependence on TMP and because approximately 50% of the TMP is believed to be consumed by this pathway, the composite TMP order should be around 1.25.

Radiolytic Studies. Radiolytic one-electron oxidation of 1,2,5-trimethylpyrrole was carried out in aqueous solutions and in organic solvents, utilizing several radicals as the oxidants. Radiolysis of N_2O-saturated aqueous solutions leads to production of •OH radicals and a small yield of H atoms. The •OH radical is known to add to pyrroles[33] very rapidly. To prevent this addition and bring about a one-electron oxidation reaction, we added 0.1 mol L^{-1} of Br^-, I^-, or N_3-. These anions react rapidly with •OH radicals to form $Br_2^{\bullet-}$, $I_2^{\bullet-}$, and $N_3^\bullet$ radicals, which are known to react as one-electron oxidants.[34] From the rate of decay of the absorptions of $Br_2^{\bullet-}$ at 360 nm and of $I_2^{\bullet-}$ at 380 nm as a function of [TMP], we derived second-order rate constants of $(2.3 \pm 0.3) \times 10^9$ L mol^{-1} s^{-1} for $Br_2^{\bullet-}$ and $(5.1 \pm 0.6) \times 10^8$ L mol^{-1} s^{-1} for $I_2^{\bullet-}$. The rate constant for $N_3^\bullet$ radicals was not determined because the absorbances of this radical and of that produced from TMP are both in the UV region and somewhat overlapping. However, since the reduction potential of the couple $N_3^\bullet/N_3^-$ (1.33 V vs NHE)[35] lies between the potentials for $Br_2^{\bullet-}/2Br^-$ (1.62 V) and $I_2^{\bullet-}/2I^-$ (1.03 V) and since $N_3^\bullet$ is known to oxidize many compounds more rapidly than $Br_2^{\bullet-}$, we conclude that k_{12} must be $> 2 \times 10^9$ L

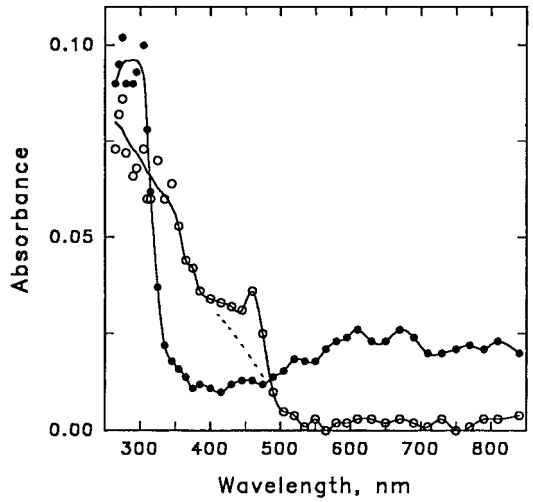

Figure 1. Optical absorption spectra recorded by pulse radiolysis of N_2O-saturated aqueous solutions containing 0.1 mol L^{-1} N_3^- and 1×10^{-3} mol L^{-1} TMP at pH 7.8, recorded 1 μs (●) and 500 μs (○) after the pulse.

mol^{-1} s^{-1}. Therefore, the oxidation of 1×10^{-3} mol L^{-1} TMP by $N_3^{\bullet}$ is expected to be practically complete within 1 μs.

$$N_3^{\bullet} + TMP \rightarrow TMP^{\bullet+} + N_3^- \qquad (12)$$

The absorption spectrum observed by pulse radiolysis of N_2O-saturated aqueous solutions containing 0.1 mol L^{-1} NaN_3 and 1×10^{-3} mol L^{-1} TMP at pH 7.8, recorded 1 μs after the pulse (Figure 1), can be ascribed to the radical cation of TMP. The spectrum has a narrow UV band, with an apparent peak at ~280 nm, and a very broad band in the visible range. The molar absorptivity of the latter band is relatively low; a value of $\epsilon = 340 \pm 30$ L mol^{-1} cm^{-1} at 650 nm was estimated from thiocyanate dosimetry.[36] The UV band has $\epsilon \sim 1300$ L mol^{-1} cm^{-1}. An earlier report[37] indicated a peak at 800 nm for the radical cation of pyrrole in an irradiated mixed-Freon glassy matrix but no further details were presented.

Figure 1 also shows that the spectrum of the radical cation changes within 500 μs to a different spectrum, with absorption only below 500 nm. This transformation follows second-order kinetics and presumably involves the dimerization of two radical cations. The formation of this dimer can be readily followed at 350 nm, and from the kinetics at different initial radical concentrations (different dose/pulse), a rate constant of $2k \sim 5 \times 10^8$ L mol^{-1} s^{-1} was estimated.

$$2TMP^{\bullet+} \rightarrow (TMP)_2 + 2H^+ \qquad (13)$$

Dimerization occurs by C−C bond formation between the two rings and loss of two protons to form the stable aromatic dimer. These two steps were not distinguishable in our experiments; possibly the deprotonation is fast as it may be effected by the azide ion acting as a base. Dimerization is likely to occur by binding at the β-positions since the α-positions are sterically hindered by the methyl groups and are not capable of rearomatizing by loss of protons. When the formation of the dimer is followed in the region of 420−470 nm, instead of 350 nm, the kinetics are found to be wavelength dependent and a slower formation process becomes apparent. This slow process was found to lead to formation of a stable product with a peak at 460 nm. The same product was observed following γ-irradiation of the same solution and will be discussed below.

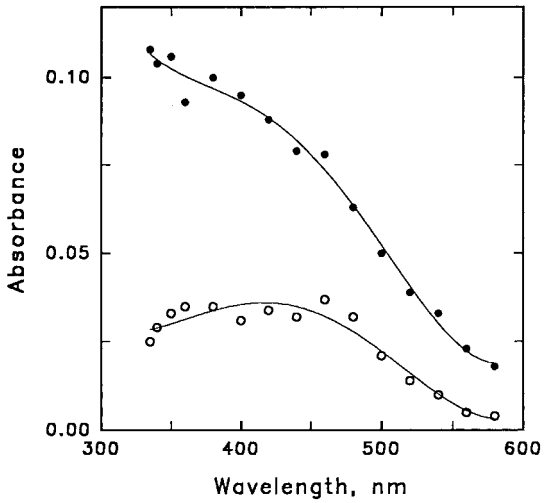

Figure 2. Optical absorption spectra recorded by pulse radiolysis of aerated CCl_4 solutions containing 2×10^{-3} mol L^{-1} TMP, recorded 1 μs (●) and 8 μs (○) after the pulse.

TMP was also oxidized in aqueous solutions by the $CCl_3O_2^{\bullet}$ radical, produced in irradiated solutions containing 2-PrOH (1.3 mol L^{-1}) and CCl_4 (5×10^{-3} mol L^{-1}) under air, with a rate constant of $(5 \pm 2) \times 10^8$ L mol^{-1} s^{-1}.

$$CCl_3O_2^{\bullet} + TMP \rightarrow CCl_3O_2^- + TMP^{\bullet+} \qquad (14)$$

The transient spectrum monitored with such solutions exhibits a UV absorption similar to that observed upon oxidation by $N_3^{\bullet}$, but the absorbance in the visible range was much smaller, only ~20%. A possible interpretation of this low absorbance is that reaction 14 accounts for only ~20% of the $CCl_3O_2^{\bullet}$ radicals, while the majority of these radicals react with TMP via addition, in agreement with earlier findings on the reaction of $CCl_3O_2^{\bullet}$ with indole.[38]

$$CCl_3O_2^{\bullet} + TMP \rightarrow CCl_3O_2{-}TMP^{\bullet} \qquad (15)$$

Radiolytic oxidation of TMP was also carried out in organic solvents. Irradiation of many organic compounds in CH_2Cl_2 and CCl_4 solutions has been shown to lead to production of one-electron-oxidized species and other products via several mechanisms.[39,40] Pulse radiolysis of CCl_4 solutions of 2×10^{-3} mol L^{-1} TMP under air resulted in the formation of a species with a very broad absorption, $\lambda_{max} \leq 320$ nm and tailing down to 600 nm (Figure 2). The absorption was formed within 1 μs after the pulse and decayed within ~5 μs; it was not observed in the absence of TMP and was negligibly small at 2×10^{-4} mol L^{-1} TMP. This broad absorption may be ascribed to a π-complex of Cl atoms[41] with TMP, similar to the complexes of Cl atoms with aromatic compounds[42] and with pyridine,[43] although the increasing absorbance in the UV may be due to the presence of another short-lived intermediate. Both of these species decay rapidly; the π-complex yields either $TMP^{\bullet+}$ and Cl^- or the σ-bonded TMP·Cl adduct. The spectrum recorded 8 μs after the pulse (Figure 2) is different and less intense than that observed immediately after the pulse. This spectrum includes the contributions of any radical cations and adducts produced from the initial π-complex as well as of the species produced by reaction of $CCl_3O_2^{\bullet}$ with TMP. The absorptions of these species in the UV could not be observed because the solutions used were not sufficiently transparent below 320 nm.

Similar experiments with TMP ($\leq 10^{-3}$ mol L^{-1}) in CH_2Cl_2 did not show formation of the Cl complex, because Cl atoms

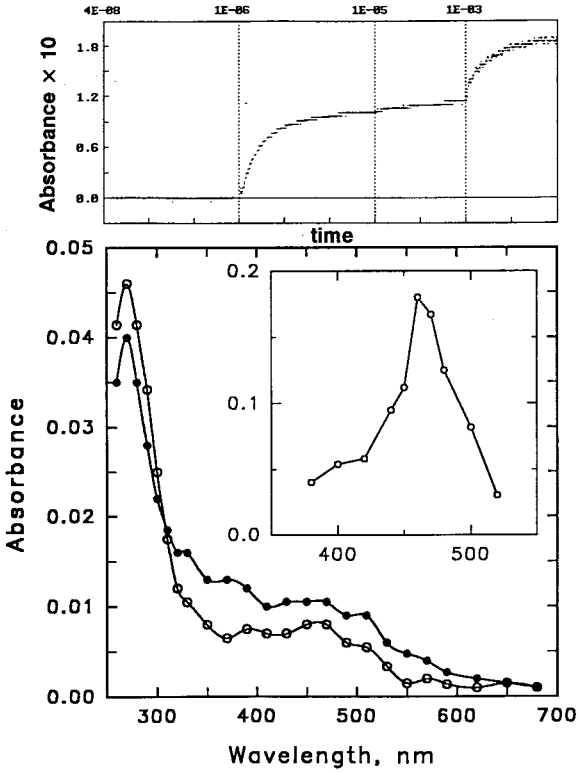

Figure 3. Optical absorption spectra recorded by pulse radiolysis of aerated CH_2Cl_2 solutions containing 2.5×10^{-4} mol L^{-1} TMP, recorded 6 μs (●) and 50 μs (○) after the pulse. The inset shows the spectrum recorded after 400 ms. The kinetic trace above the spectrum shows the growth of the 460 nm absorbance, recorded with [TMP] $= 5 \times 10^{-3}$ mol L^{-1}, as a function of time, at 4 time sections (available with the Tektronix 7612 digitizer): the first section lasts 24 μs, partly before the pulse and partly after the pulse, the small absorbance at this time scale is not visible in this section, the second section covers the following 600 μs and shows substantial growth, the third section covers the following 4 ms and shows little growth, and the fourth section covers the following 400 ms and shows a slower growth process.

react rapidly with this solvent,[39] but the reaction of the peroxyl radicals with TMP was observed. From the dependence of the formation kinetics at 400 nm on the concentration of TMP (1×10^{-4} to 1×10^{-3} mol L^{-1}) we derived a rate constant of $(1.6 \pm 0.2) \times 10^9$ L mol^{-1} s^{-1}. This is ascribed to the reaction of $CHCl_2O_2^{\bullet}$ with TMP, to form the $TMP^{\bullet+}$ radical cation and/or the adduct. The other peroxyl radical formed in this system, $CH_2ClO_2^{\bullet}$, is expected to react more slowly and its reaction may overlap the subsequent processes observed in this system. The spectrum of the transient species (Figure 3) exhibits a UV absorption with $\lambda_{max} \sim 270$ nm, similar to that observed in aqueous solutions, but the absorption in the visible range is different; it is mainly at 400−500 nm (Figure 3) instead of 600−800 nm (Figure 1). This difference may be the result of formation of different species, i.e., adducts vs radical cations, but it may be due also to the medium effect on the radical cation spectrum. The transient spectrum changes within 50 μs (Figure 3) in a complex process. An increase in absorbance was found in the range 300−600 nm, but the rate of formation was different at different wavelengths. In the 300−360 nm region the formation was complete within 100 μs, but in the 400−500 nm region the absorbance continued to grow for many milliseconds. The first process is probably a dimerization reaction similar to that observed in aqueous solutions and is expressed in the formation of absorption at the 300−360 nm region. It was difficult to derive the kinetics for this process because the absorbance changes observed are relatively small. The slower process results in a product absorbing much more intensely, with λ_{max} at 460 nm (Figure 3 inset). The slower process was monitored at 460 nm and found to continue for many milliseconds and to proceed in two steps; one step is complete within ~4 ms and the other continues for ~400 ms (kinetic trace at top of Figure 3). The spectrum monitored at both times is the same and is identical with the spectrum of the stable product observed following γ-radiolysis of a similar solution. This final product must be the result of further oxidation of the dimer. The dimer is formed within ~100 μs and may be oxidized by the $CH_2ClO_2^{\bullet}$ peroxyl radicals (since these react with TMP rather slowly and may survive until some dimer is formed). The slowest step of the 460 nm product formation may be due to oxidation of the dimer by O_2 or by hydroperoxides formed by other reactions in this system.

Gamma radiolysis of all the above solutions led to production of a stable product absorbing at 460 nm. The exact position of this peak shifted by several nanometers during the irradiation, as more of the initial TMP was oxidized. Furthermore, other peaks were observed and were different in different solvents, probably due to different products formed in addition to the predominant product. The product of irradiation in CH_2Cl_2 exhibits only the 460 nm peak and a UV absorption < 290 nm similar to that of TMP. The products in aqueous 2-PrOH/CCl_4 solutions have a peak at 460 nm and another one of similar intensity at 330 nm, but the growth profiles of the two peaks during the irradiation are slightly different. The products in N_2O-saturated aqueous solutions containing azide also have a 460 nm peak, but another broad absorption in the UV with a maximum near 300 nm is also pronounced; again the profile of growth of absorbance with dose is different for the two peaks. In contrast, irradiation of TMP in cyclohexane solutions under air forms products with only a very weak absorption at 460 nm and a higher one at 290 nm. When CCl_4 is added to the cyclohexane, the relative yield of the product absorbing at 460 nm increases by about an order of magnitude. From these results we conclude that the peak at 460 nm is formed by oxidation, whereas the other peaks may be due to various adducts. Despite the different mechanisms involved, all radiolytic product formation in aerated solutions nearly ceased when the O_2 is depleted and resumed when more O_2 was introduced into the solution.

To examine the structure of the 460 nm product, we prepared a larger quantity by irradiation of TMP in CH_2Cl_2, evaporated the solvent, and analyzed the crude product by proton NMR. In $CDCl_3$ three distinct methyl singlets were observed at 2.29, 2.85, and 3.59 ppm relative to tetramethylsilane. The chemical shift for the methyl protons in 1,2,5-trimethylpyrrole are 2.10 and 3.27 ppm (CCl_4).[44] We propose that the downfield shift observed for the methyl protons in the 460 nm product is consistent with inductive effects associated with salt formation. These findings lead us to tentatively identify the 460 nm product as the dimeric dication depicted in Scheme 1. The adducts have not been analyzed and are probably a mixture of various monomeric and dimeric products. Irrespective of mechanism, it is clear that TMP consumes O_2 readily and can deplete all the O_2 present in solution by various processes initiated by free-radical reactions. In halogenated or polar solvents TMP is readily oxidized to the radical cation, which does not react with O_2, but undergoes dimerization and further oxidation. In hydrocarbon solvents, the mechanism appears to involve mainly adduct formation. Such adducts are likely to react with O_2 to form TMP-derived peroxyl radicals, which will undergo subsequent reactions to form various oxygenated products.

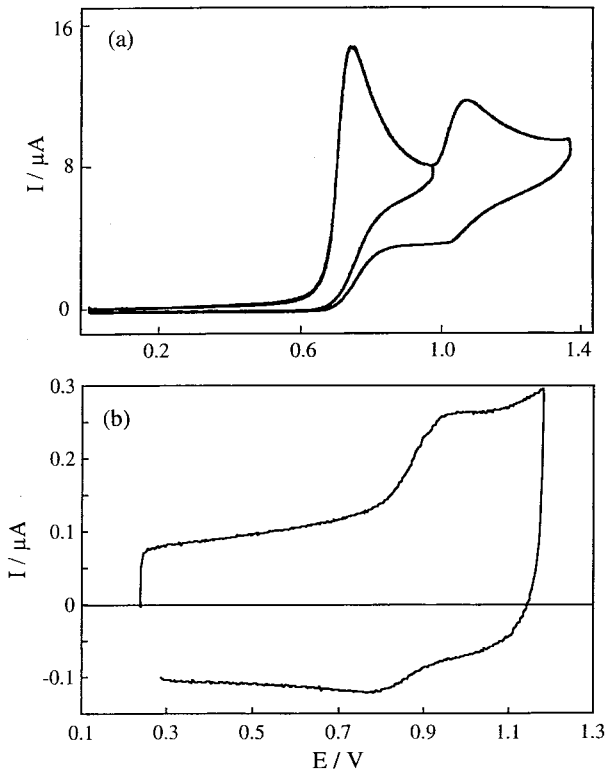

Figure 4. Cyclic voltammetry of acetonitrile solutions containing 2 $\times$ 10^{-3} mol L^{-1} TMP and 0.2 mol L^{-1} NEt_4BF_4: (a) on a 1.1 mm diameter carbon electrode (scan rate 0.2 V s^{-1}); (b) on a 10 μm diameter platinum ultramicroelectrode (scan rate 9,000 V s^{-1}). T = 20 °C.

The radiolytic yield (G value) of the oxidation of TMP was examined in CH_2Cl_2 solutions, where the conversion of TMP to the product appears to be the most direct. The yield was found to be $G = 2.3$ μmol J^{-1} at [TMP] = 3.7 $\times$ 10^{-4} mol L^{-1} and $G = 5.6$ μmol J^{-1} at [TMP] = 3.7 $\times$ 10^{-3} mol L^{-1}. Since the total yield of oxidizing species in CH_2Cl_2 is only $\sim$0.7 μmol J^{-1},[39] the measured yields for TMP oxidation indicate that a short chain reaction operates in this system. The most likely mechanism is that some of the intemediates formed from TMP react with O_2 to form peroxyl radicals, which then oxidize another molecule of TMP (Scheme 2). The initial radical cation, $TMP^{\bullet+}$, was not found to react with O_2 in the pulse radiolysis experiments, although a slow reaction under low radical concentrations cannot be ruled out.

Electrochemical Studies. To complement the above radiolytic studies, we examined the oxidation of TMP by cyclic voltammetry in acetonitrile solutions on gold and carbon electrodes. A similar electrochemical behavior was observed on the two types of electrodes. At low scan rates, an irreversible peak is observed (E_p = 0.72 V vs SCE at a scan rate of 0.2 V s^{-1} and initial concentration of 2 $\times$ 10^{-3} mol L^{-1}) (Figure 4a). This process was found to be monoelectronic by comparison with the reversible oxidation wave of ferrocene. A value of one electron per TMP was also determined by exhaustive electrolysis at 0.9 V vs SCE of a solution of 8 $\times$ 10^{-3} mol L^{-1} TMP. This peak is followed by a second partially reversible peak at a more positive potential (E° = 1.1 V). During repetitive scanning, no new peak that could be ascribed to the formation of a polymer or longer oligomers were observed at lower potential, contrary to the behavior of the unsubstituted pyrrole. To determine the kinetic behavior of the first oxidation process, the peak potential was studied as a function of the scan rate and the initial concentration of TMP. The variation of E_p with the scan rate was found to be linear, with a slope of 20.3 mV per 10-fold increase in the scan rate. A linear dependence was also found for the variation of E_p with the initial concentration of monomer, -20 mV per 10-fold increase in concentration. These results are in agreement with a mechanism involving a rapid electron transfer to form $TMP^{\bullet+}$ followed by a fast coupling between two radical cations.[45] By use of ultramicroelectrodes (with diameter in the 10 μm range), scan rates up to 10^5 V s^{-1} can be reached, allowing detection of the very short-lived radical cations of pyrroles.[46] With such techniques, and by increasing the scan rate above 5000 V s^{-1} (at 2 $\times$ 10^{-3} mol L^{-1} TMP), partial reversibility was observed (Figure 4b). In these experiments, the second, more positive peak disappeared, indicating that this peak is related to the oxidation of the product formed after the first oxidation process. The standard oxidation potential for the $TMP/TMP^{\bullet+}$ couple can be directly derived from the half-sum between the forward and reverse peak potentials. A value of 0.87 $\pm$ 0.01 V vs SCE was found. The lowest scan rate required to observe a partially reversible wave is a measure of the radical cation lifetime, and if the mechanism is known, these values can be converted to rate constants by comparison with simulated voltammograms. A second-order rate constant of $2k = (1-2) \times 10^8$ L mol^{-1} s^{-1} was estimated for the decay of $TMP^{\bullet+}$.

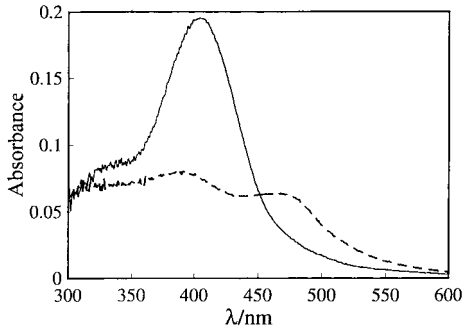

Figure 5. Spectroelectrochemistry of acetonitrile solutions containing 5 mol L^{-1} TMP and 0.2 mol L^{-1} NEt_4BF_4 in a LIGA cell. Oxidation was carried out at the potential of the first wave (solid line) and the second wave (dashed line) (see text); the curves were recorded 10 s after the potential step.

To obtain spectral information and to identify the different intermediates involved in the oxidation steps, in situ spectroelectrochemical experiments were carried out in acetonitrile during slow scan cyclic voltammetry. This technique is based on the use of electrodes with gold-LIGA structure (electrodes with honeycomb holes with diameters of 20 μm). The transmission of light through these electrodes yields spectroscopic information on the electrochemical process, and it is possible to record UV$-$visible spectra while oxidizing the TMP. This method permits recording of spectra of intermediates under complete conversion conditions on a time scale on the order of 2 s. When the oxidation potential is stepped to the level of the first oxidation wave, a large increase of the absorbance is observed in the visible range with a peak at 404 nm. This peak shifted to a higher wavelength ($\sim$420 nm) when the potential is maintained at this value. When a more positive potential is applied after standing at the level of the first oxidation process, the main peak disappears and only a broad peak at 350$-$380 nm is observed. When the potential is directly stepped to the level of the second wave, two peaks are visible at $\sim$380 and $\sim$470 nm (Figure 5). The ratio between the two peaks is different in each experiment, indicating the formation of at least two different species.

There are no data on the oxidation of 3,3′-bipyrrole, but its oxidation potential can be estimated from the values for 2,2′-

bipyrrole in acetonitrile. The $E°$ values for the oxidation of 2,2′-bipyrrole, 5-methyl-2,2′-bipyrrole, and 5,5′dimethyl-2,2′-bipyrrole have been determined to be 0.60, 0.46, and 0.30 V vs SCE,[26] respectively, indicating a decrease of ~0.15 V per methyl group. Assuming that $E°$ for the oxidation of 2,2′- and 3,3′-bipyrrole is in the same range, the oxidation potential for $(TMP)_2$ should be below 0 V/SCE (the methyl substitution on nitrogen will also decrease the oxidation potential); that is it should be very easy to oxidize this dimer. A monoelectronic wave is observed at low scan rates, indicating that the final bipyrrole is not formed on this time scale. The same behavior was previously observed for the oxidation of 2,2′-bipyrrole or 5-methyl-2,2′-bipyrrole and is due to a low rate of deprotonation of the protonated dimer in acetonitrile.[26,47,48] It is likely that the deprotonation reaction of the 3,3′-bipyrrole is also slow. Thus, the second oxidation peak observed at low scan rate voltammetry can be ascribed to the oxidation of the protonated dimer as proposed for 2,2′-bipyrrole.[48] The UV−visible spectra recorded simultaneously show absorbances around 400 nm which can be ascribed to the protonated dimers or, more likely, to evolution of these protonated dimers because their further oxidation does not lead to the same spectra as the direct oxidation at the potential of the second wave. It is noticeable that the absorption peak at 460 nm (which indicates the formation of the $\beta-\beta$ branched compound) is mainly observed when the oxidation is performed directly at the potential of the second oxidation wave. This behavior could be explained by an assistance of the deprotonation reactions of the protonated dimer by the second electron transfer, which will favor the $\beta-\beta$ coupling versus the other reaction pathways (such as reversible $\alpha-\alpha$ coupling or nucleophilic attack of the protonated dimer).

Conclusion

The results of the pulse radiolysis and electrochemical studies of the oxidation of TMP are consistent with rapid coupling of the $TMP^{\bullet+}$ radical cation and subsequent oxidation of the dimer to form a highly conjugated product that absorbs at ~460 nm. The radiolysis studies further indicate that other products are also formed, probably via reactions of peroxyl radicals. These results, when coupled with the mechanistic proposal in Scheme 1, allow us to speculate concerning the thermodynamics of the ETIO process. Step 2 is rate limiting and is likely endothermic even at 131 °C. To account for the observed TMP autoxidation, k_3 and k_5 must be competitive with k_{-2}. In apolar solvents, such as CH_2Cl_2 and chlorobenzene, the likelihood of formation of SSIP and free ions is relatively low. We propose that ion pair dynamics in our system is such that k_6 and subsequent reaction(s) are allowed to pull the ETIO reaction toward completion. Future work is planned to further elucidate the role of ion pair dynamics in autoxidation.

Appendix: Derivation of the Rate Law for Autoxidation of 1,2,5-Trimethylpyrrole (TMP) by the Peroxyl Radical Chain Depicted in Scheme 2

We start by making three assumptions.

(i) We make the standard assumption of steady-state kinetics, namely, that the rate of initiation, R_i, equals the rate of termination,

$$R_i = k_{10a}[TMPOO^{\bullet}]^2 + k_{10b}[TMPOO^{\bullet}][TMP^{\bullet}] + k_{10c}[TMP^{\bullet}]^2 \quad (16)$$

(ii) We assume that the TMP radical is relatively stable and that, at the temperature of 131 °C, step 8 is reversible with the value of its K_{eq} approaching unity,

$$k_8[TMP^{\bullet}][O_2] = k_{-8}[TMPOO^{\bullet}] \quad (17)$$

(iii) We assume that step 9 is the rate-limiting step.

Rewritting eq 17 in the form $[TMPOO^{\bullet}] = k_8/k_{-8}[TMP^{\bullet}][O_2]$ and inserting into eq 16 yields

$$R_i = k_{10a}[TMPOO^{\bullet}]^2 + \{k_8k_{10b}/k_{-8}\}[TMP^{\bullet}]^2[O_2] + k_{10c}[TMP^{\bullet}]^2 \quad (18)$$

which can be algebraically rewritten as

$$R_i = k_{10a}[TMPOO^{\bullet}]^2 + (k_8k_{10b}[O_2] + k_{-8}k_{10c})k_{-8}^{-1}[TMP^{\bullet}]^2 \quad (19)$$

From eq 17 we have

$$[TMP^{\bullet}]^2 = \{k_{-8}^2/k_8^2[O_2]^2\}[TMPOO^{\bullet}]^2 \quad (20)$$

which when inserted into eq 19 followed by rearrangement yields

$$R_i = (\{k_{10a}k_8^2[O_2]^2 + k_{10b}k_8k_{-8}[O_2] + k_{-8}^2k_{10c}\}/k_82[O_2]^2)[TMPOO^{\bullet}]^2 \quad (21)$$

Solving for $[TMPOO^{\bullet}]$ yields

$$[TMPOO^{\bullet}] = k_8[O_2]R_i^{1/2}/\{k_{10a}k_8^2[O_2]^2 + k_{10b}k_8k_{-8}[O_2] + k_{-8}^2k_{10c}\}^{1/2} \quad (22)$$

Since the rate-limiting step is step 9,

$$-d[TMP]/dt = k_9[TMPOO^{\bullet}][TMP] \quad (23)$$

substitution of eq 22 into eq 23 yields

$$-d[TMP]/dt = k_9k_8R_i^{1/2}[TMP][O_2]/(k_{10a}k_8^2[O_2]^2 + k_{10b}k_8k_{-8}[O_2] + k_{10c}k_{-8}^2)^{1/2} \quad (24)$$

As discussed in the text, the mechanisms depicted in Schemes 1 and 2 are intimately related. It is proposed that Scheme 1 provides the initiation for the peroxyl chain mechanism depicted in Scheme 2. That is that the R_i term in the peroxyl chain mechanism is derived from the slow step in Scheme 1, step 2. Thus,

$$R_i = K_1K_2[TMP][O_2] \quad (25)$$

and

$$R_i^{1/2} = K_1^{1/2}K_2^{1/2}[TMP]^{1/2}[O_2]^{1/2} \quad (26)$$

Substituting into eq 24 yields eq 11,

$$-d[TMP]/dt = k_9K_1^{1/2}K_2^{1/2}[TMP]^{3/2}[O_2]^{3/2}/\{k_{10a}k_8^2[O_2]^2 + k_{10b}k_8k_{-8}[O_2] + k_{10c}k_{-8}^2\}^{1/2} \quad (11)$$

References and Notes

(1) Beaver, B. D.; Cooney, J. V.; Watkins, J. M., Jr. *Heterocycles* **1985**, *23*, 2847; *J. Heterocycl. Chem.* **1986**, *23*, 1095.

(2) Beaver, B. D.; Treaster, E.; Kehlbeck, J. D.; Martin, G. S. *Energy Fuels* **1994**, *8*, 455.

(3) Ali, M. F.; Hamdan, A. J.; Nizami, A. PREPRINTS **1994**, *39*, 67.

(4) Ingold, K. U. In *Free Radicals*; Kochi, J. K., Ed.; Wiley-Interscience: New York, 1973; pp 37−112.

(5) Beaver, B. D.; Hazlett, R. N.; Cooney, J. V.; Watkins, J. M., Jr. *Fuel. Sci. Technol. Int.* **1988**, *6*, 131. Beaver, B. D. *Fuel Sci. Technol. Int.* **1991**, *9*, 1287.

(6) Beaver, B.; DeMunshi, R.; Heneghan, S. P.; Whitacre, S. D.; Neta, P. *Energy Fuels* **1997**, *11*, 396.

(7) Alfassi, Z. B.; Neta, P.; Beaver, B. *J. Phys. Chem. A* **1997**, *101*, 2153.

(8) *Handbook of Conducting Polymers*; Skotheim, T. A., Ed.; Marcel Dekker: New York, 1986; Vol. 1.

(9) Andrieux, C. P.; Hapiot, P.; Audebert, P.; Guyard, L.; Nguyen Dinh An, M.; Groenendaal, L.; Meijer, E. W. *Chem. Mater*. **1997**, *9*, 723. Audebert, P.; Guyard, L.; Nguyen Dinh An, M.; Hapiot, P.; Chahma, M.; Combelas, C.; Thiebault, A. *J. Electroanal. Chem.* **1996**, *407*, 169, and references therein.

(10) Avila, D. V.; Davies, A. G. *J. Chem. Soc., Faraday Trans.* **1990**, *86*, 3243. Davies, A. G.; Julia, L.; Yazdi, S. N. *J. Chem. Soc., Perkin Trans. 2* **1989**, 239. Shiotani, M.; Nagata, Y.; Tasaki, M.; Sohma, J.; Shida, T. *J. Phys. Chem.* **1983**, *87*, 1170. Rao, D. N. R.; Symons, M. C. R. *J. Chem. Soc., Perkin Trans. 2* **1983**, 135.

(11) Dos Santos, D. A.; Brédas, J. L. *J. Chem. Phys.* **1991**, *95*, 6567.

(12) Becke, A. D. *J. Chem. Phys.* **1993**, *98*, 5648.

(13) Hariharan, P. C.; Pople, J. A. *Chem. Phys. Lett.* **1972**, *16*, 217.

(14) Frisch, M. J.; Trucks, G. W.; Schlegel, H. B.; Gill, P. M. W.; Johnson, B. G.; Robb, M. A.; Cheeseman, J. R.; Keith, T.; Petersson, G. A.; Montgomery, J. A. Raghavachari, K.; Al-Laham, M. A.; Zakrzewski, V. G.; Ortiz, J. V.; Foresman, J. B.; Cioslowski, J.; Stefanov, B. B.; Nanayakkara, A.; Challacombe, M.; Peng, C. Y.; Ayala, P. Y.; Chen, W.; Wong, M. W.; Andres, J. L.; Replogle, E. S.; Gomperts, R.; Martin, R. L.; Fox, D. J.; Binkley, J. S.; Defrees, D. J.; Baker, J.; Stewart, J. P.; Head-Gordon, M. Gonzalez, C.; Pople, J. A. *Gaussian 94, Revision E.1*; Gaussian, Inc., Pittsburgh, PA, 1995.

(15) Tschuncky, P.; Heinze, J.; Smie, A.; Engelmann, G.; Kobmehl, G. *J. Electroanal. Chem.* **1997**, *433*, 225.

(16) Sauvajol, J. L.; Chorro, C.; Lere-Porte, J.-P.; Moreau, J. J. E.; Thepot, P.; Wong Chi Man, M. *Synth. Met.* **1994**, *62*, 233.

(17) Hapiot, P.; Gaillon, L.; Audebert, P.; Moreau, J. J. E.; Lere-Porte, J.-P.; Wong Chi Man, M. *J. Electroanal. Chem.* **1997**, *435*, 85.

(18) The mention of commercial equipment or material does not imply recognition or endorsement by the National Institute of Standards and Technology, nor does it imply that the material or equipment identified are necessarily the best available for the purpose.

(19) Garreau, D.; Savéant, J.-M. *J. Electroanal. Chem.* **1972**, *35*, 309.

(20) Andrieux, C. P.; Garreau, D.; Hapiot, P.; Pinson, J.; Savéant, J.-M. *J. Elelectroanal. Chem.* **1988**, *243*, 321.

(21) Neudeck, A.; Dunsch L. *J. Electroanal. Chem.* **1995**, *386*, 135.

(22) Self-initiated autoxidations have been previously observed, Russell, G. A. *J. Am. Chem. Soc.* **1956**, *78*, 1041.

(23) Furimsky, E.; Howard, J. A. *J. Am. Chem. Soc.* **1973**, *95*, 369.

(24) Cooney, J. V.; Hazlett, R. N. *Heterocycles* **1984**, *22*, 1513.

(25) Masnovi, J. M.; Kochi, J. K. *J. Am. Chem. Soc.* **1985**, *107*, 7880.

(26) Guyard, L.; Hapiot,; P. Neta, P. *J. Phys. Chem.* **1997**, *101*, 5698.

(27) Andrieux, C. P.; Audebert, P.; Hapiot, P.; Savéant, J.-M. *J. Phys. Chem.* **1991**, *95*, 10158.

(28) Jin, F.; Leitich, J.; von Sonntag, C. *J. Chem. Soc., Perkin Trans. 2* **1993**, 1589.

(29) Fang, X.; Jin, F.; Jin, H.; von Sonntag, C. *J. Chem. Soc., Perkin Trans. 2* **1998**, 259.

(30) Albini, A.; Mella, M.; Freccero, M. *Tetrahedron* **1994**, *50*, 575.

(31) Sawyer, D. T.; Valentine, J. S. *Acc. Chem. Res.* **1981**, *14*, 393.

(32) Jones, R. A.; Bean, G. P. *The Chemistry of Pyrroles*; Academic Press: London, 1977; pp 219−224.

(33) Lilie, J. *Z. Naturforsch. B* **1971**, *26*, 197. Samuni, A.; Neta, P. *J. Phys. Chem.* **1973**, *77*, 1629.

(34) Neta, P.; Huie, R. E.; Ross, A. B. *J. Phys. Chem. Ref. Data* **1988**, *17*, 1027.

(35) Stanbury, D. M. *Adv. Inorg. Chem.* **1989**, *33*, 69.

(36) Schuler, R. H.; Patterson, L. K.; Janata, E. *J. Phys. Chem.* **1980**, *84*, 2088.

(37) Grimison, A.; Simpson, G. A. *J. Phys. Chem.* **1968**, *72*, 1776.

(38) Shen, X.; Lind, J.; Eriksen, T. E.; Merenyi, G. *J. Chem. Soc., Perkin Trans. 2* **1989**, 555.

(39) Alfassi, Z. B.; Mosseri, S.; Neta, P. *J. Phys. Chem.* **1989**, *93*, 1380.

(40) Grodkowski, J.; Neta, P. *J. Phys. Chem.* **1984**, *88*, 1205, and references therein.

(41) Chateauneuf, J. E. *Chem Phys. Lett.* **1989**, *164*, 577.

(42) Raner, K. D.; Lusztyk, J. Ingold, K. U. *J. Phys. Chem.* **1989**, *93*, 564.

(43) Breslow, R.; Brandl, M.; Hunger, J.; Turro, N.; Cassidy, K.; Krogh-Jesperson, K.; Westbrook, J. D. *J. Am. Chem. Soc.* **1987**, *109*, 7204.

(44) Hinman, R. L.; Theodoropulos, S. *J. Org. Chem.* **1963**, *28*, 3052.

(45) Andrieux, C. P.; Nadjo, L.; Savéant, J.-M. *J. Electroanal. Chem.* **1973**, *42*, 242.

(46) Andrieux, C. P.; Audebert, P.; Hapiot, P.; Savéant, J.-M. *J. Am. Chem. Soc.* **1990**, *112*, 2439.

(47) Niziurski-Mann, R. E.; Scordilis-Kelley, C.; Liu, T.-L.; Cava, M. P.; Carlin, R. T. *J. Am. Chem. Soc.* **1993**, *115*, 887.

(48) Zotti, G.; Schiavon, G.; Zecchin, S.; Sannicolo, F.; Brenna, E. *Chem. Mater.* **1995**, *7*, 1464.